Journal of Renewable Materials

Tech Science Press

DOI: 10.32604/jrm.2022.019491

ARTICLE

Facile Synthesis of a Novel Bio-Based P-N Containing Flame Retardant for Effectively Reducing the Fire Hazards of Epoxy Resin

Meixian Li[1], Xin Hu[1], Jie Yang[1], Hongyu Yang[1,3,*] and Yao Yuan[2,*]

[1]College of Materials Science and Engineering, Chongqing University, Chongqing, 400044, China

[2]Fujian Provincial Key Laboratory of Functional Materials and Applications, School of Materials Science and Engineering, Xiamen University of Technology, Xiamen, 361024, China

[3]State Key Laboratory of Fire Science, University of Science and Technology of China, Hefei, 230026, China

[*]Corresponding Authors: Hongyu Yang. Email: yhongyu@cqu.edu.cn; Yao Yuan. Email: yuanyao@xmut.edu.cn

Received: 27 September 2021 Accepted: 22 November 2021

ABSTRACT

In this work, a bio-based flame retardant (Cy-HEDP) was synthesized from cytosine and HEDP through a facile salt-forming reaction and embedded into epoxy matrix to improve the flame retardancy and smoke suppression performance. The product Cy-HEDP was well characterized by FTIR, ^{1}H and ^{31}P NMR and SEM tests. On the basis of the results, by adding 15 wt% Cy-HEDP, the EP_{15} can pass UL-94 V-0 rating, and the total smoke production (TSP) as well as total heat release (THR) can be decreased by 61.05% (from 22.61 to 8.7 m^2/m^2) and 39.44% (from 103.19 to 62.50 MJ/m^2) in comparison to the unfilled EP, reflecting the attenuated smoke toxicity and impeded heat generation. According to the analysis results of residual char, it can be concluded that Cy-HEDP possessed the ability to promote the formation of continuous and dense char layers, which would be a physical barrier to insulate oxygen and prevent heat feedback during the combustion of EP. This work provide inspiration towards developing bio-based flame retardant, probably extending the prospects to other polymeric material system.

KEYWORDS

Bio-based materials; cytosine; smoke suppression; flame retardant; epoxy resin

1 Introduction

As a well-popular thermosetting polymer, epoxy resin (EP) has been widely used in many fields such as adhesive [1,2], construction materials [3,4], aerospace [2,5], electrical area [6] owing to its high adhesive strength, chemical stability, mechanical properties and excellent insulation properties, etc. Unfortunately, EP exhibits high flammability and releases a large amount of toxic smoke during combustion, which causes potential hazards to human health and greatly restricts the broadening of applications [7,8]. It is vital, therefore, to improve the flame retardancy and reduce the smoke toxicity of EP composites. Generally, the incorporation of flame retardants into EP is a facile and effective way to improve its fire safety [9,10], nonetheless, the most popular flame retardants applied in the past decades are halogen-containing materials, which leads to environmental problems and unsustainability on a global scale.

To meet an increasing demand for fire-safe polymer and sustainable development, it is inevitable to replace the petroleum-based flame retardants with bio-based flame retardants. Phosphorus and

This work is licensed under a Creative Commons Attribution 4.0 International License, which permits unrestricted use, distribution, and reproduction in any medium, provided the original work is properly cited.

nitrogen-containing compounds have been recognized as a potential alternative for halogen flame retardants due to their less impact on environment and higher efficiency. Fundamentally, phosphorus and nitrogen-containing flame retardants play a role in both condensed phase and gas phase, exerting diluting effect (dilute the oxygen and inflammable gases) and charring effect (form more compact char residues), respectively. Meanwhile, phosphorus and nitrogen-containing flame retardants from bio-based materials have attracted particular interests in both the academic and industrial research owing to their practical characteristics such as low environmental impact, green source, great compatibility with polymer matrix and acceptable fire performance.

Recently, considerable efforts have been made to explore preparing flame retardants from bio-based materials, which are more sustainable than petroleum-based products due to their renewability. It has been confirmed that bio-based materials are desirable raw materials for flame retardants, e.g., cellulose [11], gluconate [12], phytic acid [13–15], chitosan [16], cytosine [17], lignin [18], starch [19] due to the rich terminal groups that provide active sites for covalent or non-covalent functionalization. Yu et al. [17] have synthesized a bio-based flame retardant (PPA-C) through cytosine and pyrophosphate, and compounded it with pentaerythritol (PER) to improve the flame retardancy of polypropylene. UL-94 V-0 rating was achieved with the incorporation of 18 wt% PPA-C/PER (3:1). Xu et al. [20] incorporated ammonium polyphosphate (APP) and a bio-based flame retardant prepared from vanillin into epoxy resin, significant reduction in heat release rate associated with UL-94 V-0 rating can be observed. Many researches showed that, a supersize portion of bio-based additives into polymer matrix present efficient flame retardancy together with synthetic materials made from fossil sources, i.e., pentaerythritol [21,22] and ammonium polyphosphate [20,23,24], but such methods usually involved complicated synthesis route and preparation process.

In this work, cytosine (Cy) used as a promising bio-based material was combined with hydroxyethylidene diphosphonic acid (HEDP) to synthesize a bio-based flame retardant based on a facile and economical synthetic method and then incorporated into epoxy matrix by solution blending. The bio-based and microscale product named Cy-HEDP was well characterized by Fourier transform infrared spectroscopy (FTIR), ^{1}H and ^{31}P nuclear magnetic resonance (NMR), scanning electronic microscopy (SEM) as well as X-ray photoelectron spectroscopy (XPS). The thermal stability of EP/Cy-HEDP composites was measured by thermogravimetry analysis (TGA). The flame retardancy of EP/Cy-HEDP composites was investigated by limiting oxygen index (LOI), vertical burning (UL-94) test and cone calorimeter test (CCT). Furthermore, the possible mechanism for achieving of fire hazards suppression was analyzed by SEM, TG-IR and Raman spectroscopy.

1.1 Materials

Polymer matrix was adopted as bisphenol-A type EP (DGEBA, E-44) with epoxide equivalent of 0.44, which was provided by SINOPEC Group Co., Ltd., China. 4, 4'-diaminodiphenylmethane (DDM), hydroxyethylidene diphosphonic acid (HEDP, 60% aqueous solution) and cytosine (Cy, powder with purity of 98%) were purchased from Adamas Reagent, LTD. Anhydrous ethanol and acetone were purchased from Chongqing Chuandong Chemical Co., Ltd. All reagents were used as received and without further purification.

1.2 Synthesis of Cy-HEDP

The Cy-HEDP was synthesized from cytosine and HEDP via a facile salt-forming reaction, as shown in Scheme 1. In the first step, 11.34 g (0.1 mol) cytosine and anhydrous ethanol (250 ml) were added into a 500 ml three-necked round-bottomed glass flask. After that, the mixed solution was heated up to 70°C and kept for 1 h under magnetic stirring. Subsequently, 17.17 g (0.05 mol) HEDP was added dropwise into the above suspension through a constant pressure dropping funnel and reacted at 70°C for 15 h with

vigorous stirring. Finally, the resulting products were obtained after being filtered, washed with anhydrous ethanol at least three times and dried in a vacuum oven. The yield was as high as 98%.

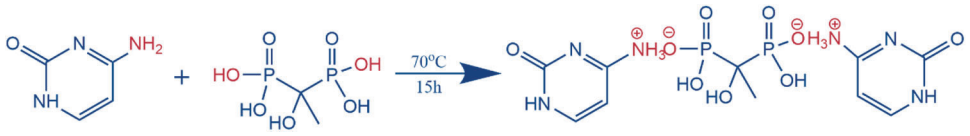

Scheme 1: The synthesis route of Cy-HEDP

1.3 Preparation of Cured EP Composites

The EP composites were prepared through a facile solution blending method [25], where the curing agent was DDM. Briefly, the preparation procedure of EP composite with 5 wt% Cy-HEDP (labeled as EP_5) was listed as follows: 8.72 g DDM was melted in an oven at 100°C for increasing its fluidity before mixing. Meanwhile, 38 g EP and 2 g Cy-HEDP were dissolved in 50 ml acetone to form a homogenous suspension. Then, the mixture was heated at 100°C with constant agitation until the acetone was completely evaporated. Finally, DDM was added into the suspension above and poured into a polytetrafluoroethylene mold, followed by curing at 120°C and 150°C for 2 h, respectively. In this work, the preparation of EP composites with 10 wt% and 15 wt% Cy-HEDP were labeled as EP_{10} and EP_{15}, respectively.

1.4 Characterizations

Fourier transform infrared (FTIR) spectroscopy was performed on a Nicolet iS50 spectrometer (Nicolet Instrument Company, U.S.) using KBr pellet method. Wavenumber ranges from 4000 to 400 cm^{-1} with 32 scans accumulated and the resolution of 4 cm^{-1}.

^{1}H and ^{31}P nuclear magnetic resonance (NMR) spectroscopy were obtained from an advance Bruker 400 M NMR spectrometer (Bruker Company, Switzerland) with Dimethyl sulfoxide-d_6 as the solvent.

The morphology of the resulting product Cy-HEDP and the residual char of EP composites after the cone calorimeter test were observed by scanning electronic microscopy (SEM, FEI Nova 400, Holland). The samples were coated with gold for 30 s.

XPS measurements were performed in an ESCALAB250Xi spectrometer using a monochromatic Al kα X-ray source.

Thermogravimetry analysis (TGA) was performed on TGA2 Thermogravimetric Analyzer (Mettler Toledo, Switzerland). About 3 mg of the sample was heated from the room temperature to 700°C under the nitrogen flow at a heating rate and gas flow rate of 20 °C/min and 50 ml/min, respectively.

The limited oxygen index (LOI) of the EP and EP/Cy-HEDP composites was measured by HC-2C oxygen index instrument (Jiangning Analysis Instrument Co., China) based on standard ASTM D2863-97 with the samples size of 100.0 mm × 6.5 mm × 3.0 mm.

UL-94 test was carried on CZF-2 vertical burning testing instrument (Jiangning Analysis Instrument Co., China) according to ASTM D3801 with the sample in the dimension of 100.0 mm × 13.0 mm × 3.0 mm.

The cone calorimeter test (CCT) was studied by an instrument of Suzhou Vouch Testing Technology Co., Ltd. in conformity with ISO 5660. Samples with the size of 100.0 mm × 100.0 mm × 3.0 mm were irradiated at a heat flow of 35 kW/m^2.

The residual char after CCT was analyzed by Raman spectroscopy, which was conducted by a LabRAM HR Evolution apparatus (Jobin Yvon Instruments, France) with a 512.5 nm argon ion laser.

Thermogravimetric analysis/infrared spectrometry (TG-IR) was performed on a TGA Q5000 thermogravimetric analyzer combined with a Nicolet 6700 FT-IR spectrophotometer via a metal

transmission pipe. The samples were heated from the room temperature to 700°C under nitrogen atmosphere at a heating rate and gas flow rate of 20 °C/min and 20 ml/min, respectively.

2 Results and Discussion

2.1 Characterization of Cy-HEDP

The composition and structure of Cy, HEDP and Cy-HEDP were determined by FTIR spectra, as portrayed in Fig. 1. The characteristic peaks of HEDP emerge at 1117, 999 and 916 cm^{-1} are assigned to the stretching vibration of –P = O, –P–O– and –P–C– [26,27], respectively. The absorption peaks appear at 3384 and 3169 cm^{-1} are ascribed to the N–H bond in Cy [28–30], and the peak for the stretching vibration of –C = N emerges at 1663 cm^{-1} [28]. As for the resulting product Cy-HEDP, the peaks at 905, 1001 and 1078 cm^{-1} are respectively caused by the –P–C–, –P = O and –P–O– stretching vibrations, indicating the presence of phosphorus-containing segments in HEDP. The peak at 1663 cm^{-1} is assigned to the absorption peak of –C = N, which suggests the successful introduction of Cy. Owing to the existence of O–H in HEDP , the peak at 3103 cm^{-1} ascribed for the vibration of N–H becomes wider. Moreover, there is a new absorption band appears at 1543 cm^{-1} for Cy-HEDP, which is ascribed to the NH_3^+ vibrational mode [31], indicating that the successful reaction between Cy and HEDP.

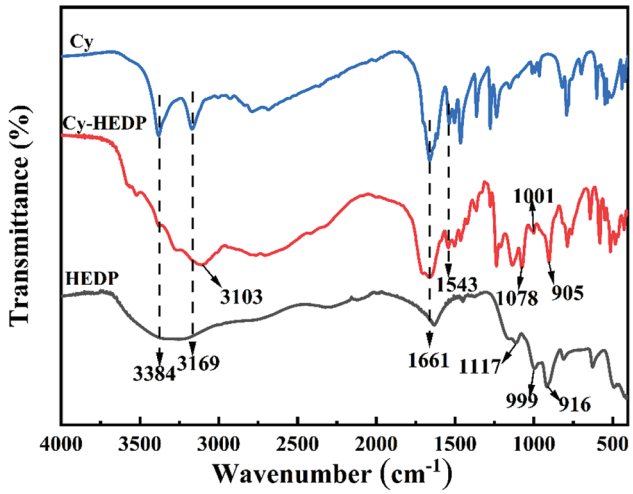

Figure 1: FTIR spectra of Cy, HEDP and Cy-HEDP

The ^1H and ^{31}P NMR were conducted to further analyze the structure of Cy-HEDP. Fig. 2 depicts the ^1H NMR spectrum of Cy-HEDP, the signals at 7.51 and 5.71 ppm are ascribed to the proton in –CH = CH– of the Cy ring. The signal at 7.51 ppm is referred to the hydrogen atom on No. 2 carbon atom, while the signal at 5.71 ppm is referred to that of No. 1 carbon atom. The chemical shift at 7.91 ppm reveals the contribution of the proton in –P–OH, while the broad peak around 6.20 ppm can be ascribed to the proton in –C–OH. The peaks around 1.4 ppm correspond to the proton in $–CH_3$ of Cy-HEDP, while the signal at 2.51 ppm is ascribed to the proton in $–CH_3$ of the solvent DMSO. As for the abnormal disappearance of amino proton signal (–NH– and $–NH_3^+$) may be caused by the solution concentration and temperature of experiment [32]. In the ^{31}P NMR, the one peak at 19.75 ppm is ascribed to the phosphorus atom of –P = O in Cy-HEDP. These results verify the successful synthesis of the target product.

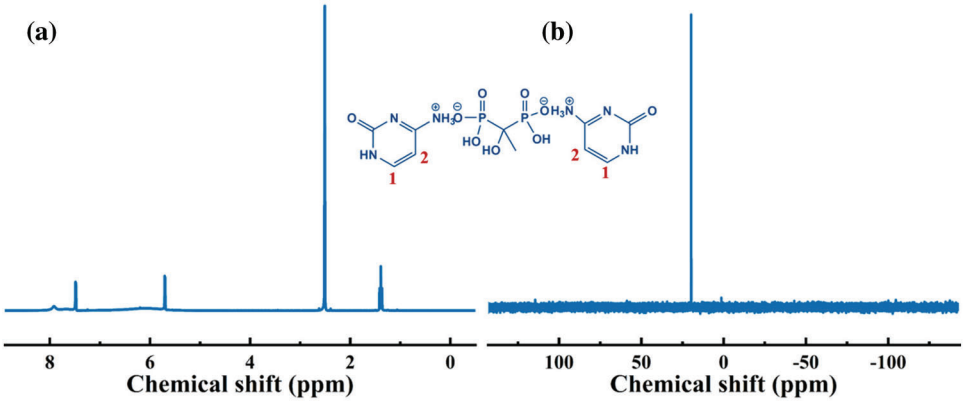

Figure 2: ^{1}H (a) and ^{31}P (b) NMR spectra of Cy-HEDP

The SEM was used to observe the morphologies of Cy and Cy-HEDP micro-particles. SEM images of Cy and Cy-HEDP are showed in Fig. 3, it is noted that Cy displays regular strip crystal with rough surface. By contrast, Cy-HEDP shows irregular lamellar crystals with smooth surface. The morphology of Cy and Cy-HEDP showed obvious differences, indicating the actual chemical reaction occurred.

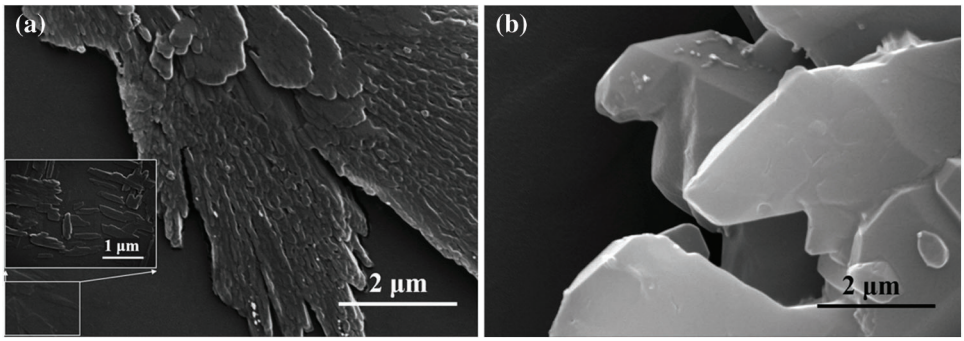

Figure 3: SEM images of Cy (a) and Cy-HEDP (b)

The XPS results (Fig. 4) depicted that there are C, N, O and P elements on the surface of Cy-HEDP. Specifically, the binding energy of O 1s located at 532.13 eV while that of N 1s occurred at 400.91 eV. The C 1s signal includes multiple peaks corresponding to C–C (284.80 eV), C–N (286.41 eV) and C = O (carbonyl, 289.01 eV). The signals appeared at 190.87 eV and 133.26 are ascribed to P 2s and P 2p, respectively. All the results above confirmed the successful reaction between HEDP and Cy.

2.2 Thermostability Analysis

The thermostability of Cy-HEDP, EP and its composites was studied by TGA test under nitrogen atmospheres and the corresponding TG and DTG curves are showed in Fig. 5. In addition, the thermal parameters, including the temperature at 5% mass loss (T_d), the temperature at maximum weight loss rate (T_{max}) and the char yield (CY) at 700°C are illustrated in Table 1. As shown in DTG curves, all samples show similar degradation behavior, where only one-stage thermal decomposition process could be observed. This is mainly due to the decomposition of the macromolecular chains [33]. Specifically, the T_d and T_{max} of EP/Cy-HEDP composites were lower than those of pure EP, which is mainly caused by the weak O = P–O and P–C–P bonds of Cy-HEDP [34]. On the other hand, the early degradation of Cy-HEDP contributes to its catalytic carbonization effect and preventing the EP matrix from further

combustion. In the case of char residues, the incorporation of Cy-HEDP can enhance the volume of residual char at high temperature. Comparing to pure EP, the residual char of EP_{15} increased from 14.6% to 23.7%, showing an increment of 62.3%, indicating the contribution of Cy-HEDP in char formation.

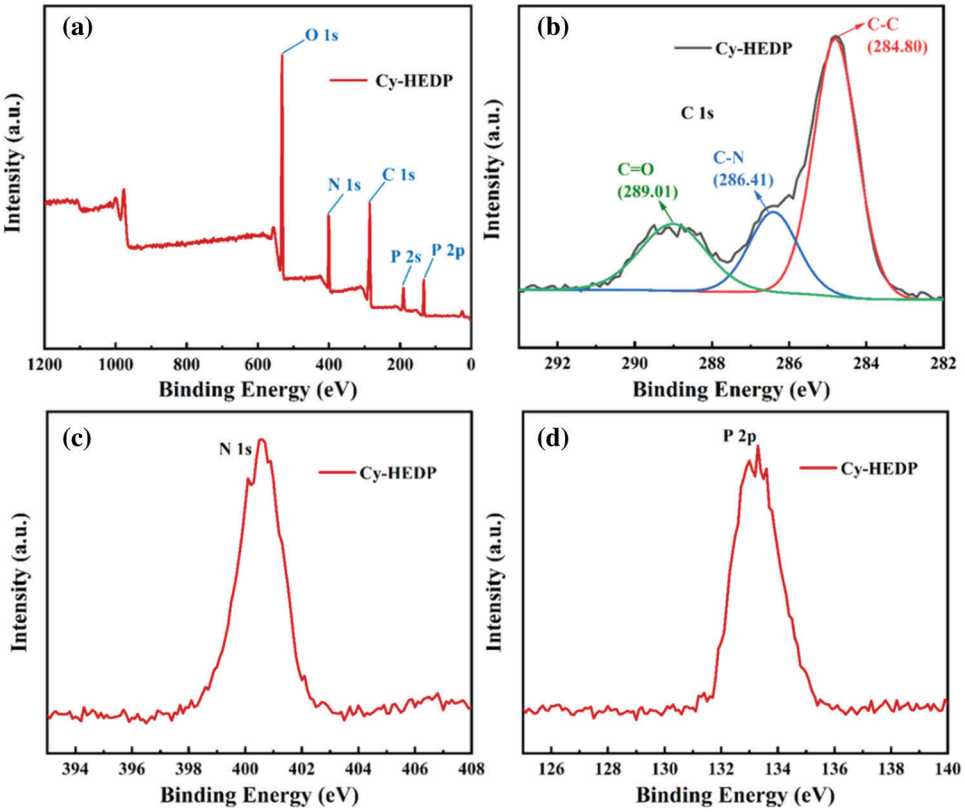

Figure 4: XPS of Cy-HEDP (a) survey spectrum; (b) C 1s; (c) N 1s; (d) P 2p

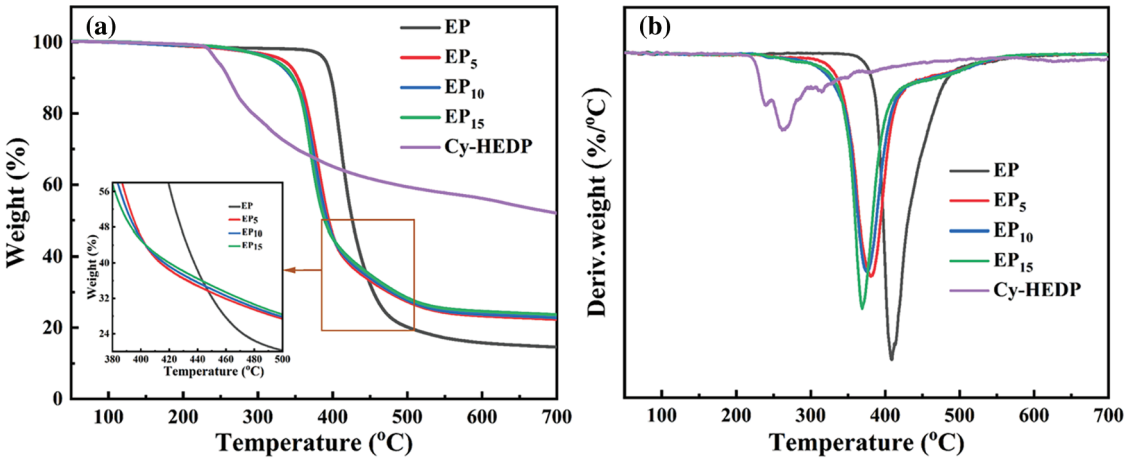

Figure 5: TG (a) and DTG (b) curves of Cy-HEDP, EP and EP/Cy-HEDP composites under nitrogen atmosphere

Table 1: Thermal stability parameters from TGA and DTG curves

Sample	T_d (°C)	T_{max} (°C)	Char yield at 700°C (%)
EP	389	408	14.6
EP_5	332	381	22.4
EP_{10}	320	376	22.9
EP_{15}	320	369	23.7
Cy-HEDP	245	263	52.0

2.3 Flame Retardancy of EP and EP/Cy-HEDP Composites

The flame-retardant effect of Cy-HEDP on EP composites was characterized by the LOI and UL-94 test, as listed in Table 2. Apparently, with the LOI value of 25.5%, the pure EP is extremely flammable, and no any UL-94 rating can be achieved. Nevertheless, with the addition of Cy-HEDP, the LOI value increased gradually. When the content of flame retardant was 5, 10 and 15 wt%, the LOI value of EP/Cy-HEDP composites rose to 26.5%, 27.0% and 28.5%, respectively. More excitedly, when 15 wt% of Cy-HEDP is incorporated, the EP_{15} composite reaches UL-94 V-0 rating during the vertical burning test. All the results above show that Cy-HEDP plays an effective role in enhancing the flame retardancy of EP.

Table 2: UL-94 and LOI data of EP and EP/Cy-HEDP composites

Sample	EP (wt%)	Cy-HEDP (wt%)	LOI (%)	UL-94 rating
EP	100	0	25.5	NR
EP_5	95	5	26.5	NR
EP_{10}	90	10	27.0	V-1
EP_{15}	85	15	28.5	V-0

2.4 Combustion Behavior of EP and EP/Cy-HEDP Composites

The cone calorimeter test (CCT) is the dependable measurement to simulate the real fire disaster [35]. It was conducted on pure EP as well as EP/Cy-HEDP composites to investigate the flame-retardant performance. The heat release rate (HRR), total heat release (THR), smoke production rate (SPR) and total smoke production (TSP) curves of EP and EP/Cy-HEDP composites are showed in Fig. 6. Furthermore, the main relevant CCT parameters including the time to ignition (TTI), THR, the peak of HRR (p-HRR), TSP, the peak of SPR (p-SPR), the average carbon monoxide yield (av-COY) and the Char residue were summarized in Table 3. The TTI results show that EP/Cy-HEDP composites can be ignited easier than pure EP, which is mainly due to the early decomposition caused by the addition of Cy-HEDP, which is in accordance with the TGA analyses. The HRR curve of pure EP presents a single strong peak with a p-HRR value of 1078.43 kW/m^2. With the addition of Cy-HEDP, the value of p-HRR was decreased significantly with the increase of Cy-HEDP content. Comparing to neat EP, the p-HRR values of EP_5, EP_{10} and EP_{15} decreased to 540.57, 438.01 and 310.93 kW/m^2, showing a decrement of 49.87%, 59.38% and 71.17%, respectively. Meanwhile, the THR values of the EP_5, EP_{10} and EP_{15} were reduced from 103.19 MJ/m^2 of pure EP to 83.53, 73.44 and 62.50 MJ/m^2 with the corresponding reduction of 19.06%, 28.83% and 39.44%, respectively.

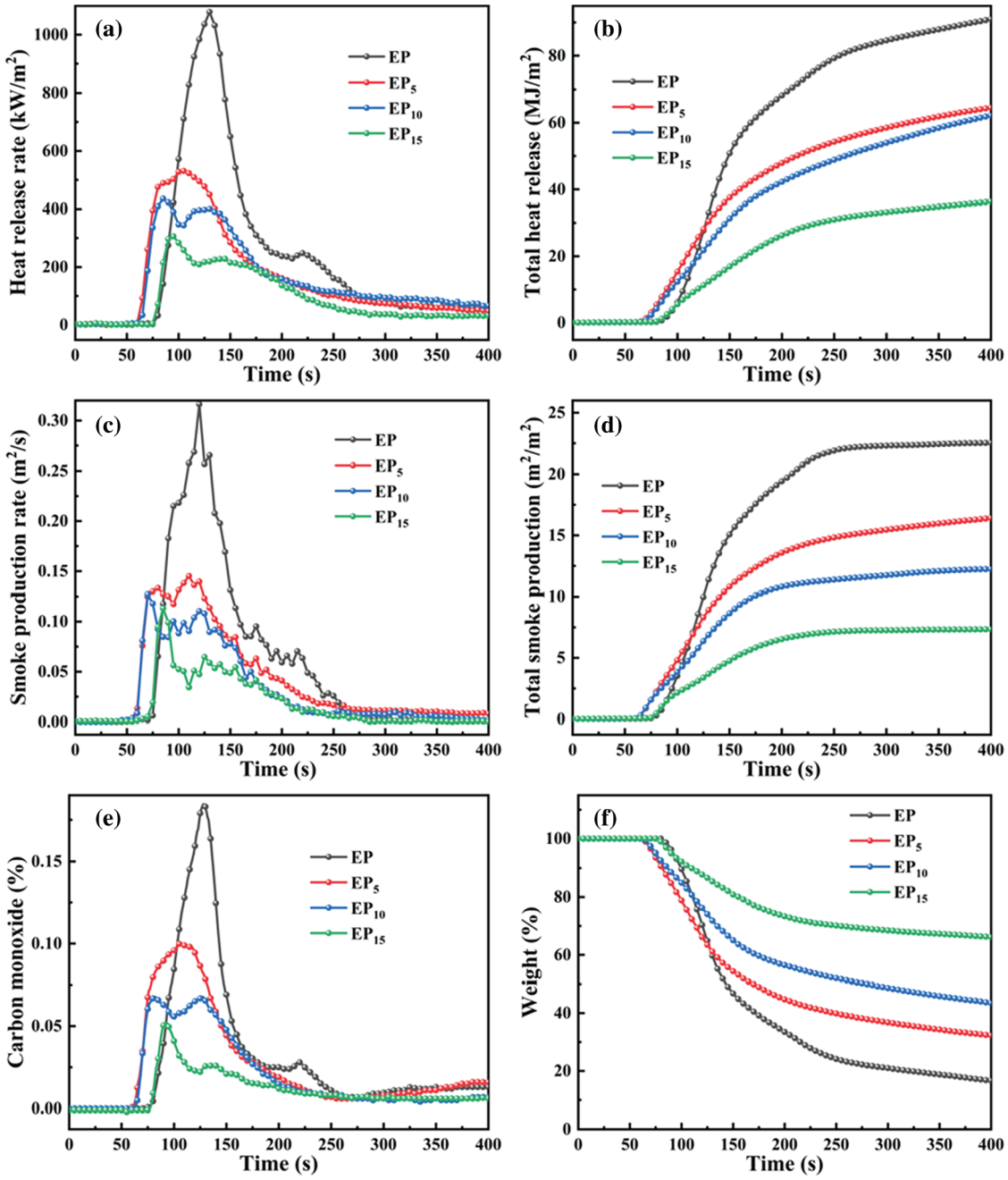

Figure 6: HRR (a), THR (b), SPR (c), TSR (d), CO (e) and weight (f) curves of EP and EP/Cy-HEDP composites

Generally, epoxy thermoset can burn rapidly and produce a larger amount of smoke and toxic fumes (especially carbon monoxide). Here, Fig. 6 displays the SPR curve of pure EP including a sharp peak (p-SPR) with the value of 0.32 m^2/s, while those of EP_5, EP_{10} and EP_{15} decreased to 0.15, 0.13, and 0.11 m^2/s, encountering a 54.11%, 59.88% and 64.30% decrement compared to pure EP, respectively. When it comes to the TSP curves, 5 wt% of Cy-HEDP shows limited impact on TSP, descending to 20.19 m^2/m^2, while that of EP reaches 22.6 m^2/m^2. When the Cy-HEDP content increases to 10 and

15 wt%, the TSP value of EP_{10} and EP_{15} get a joint decline to 12.55 and 8.7 m^2/m^2, with the corresponding decrement of 44.47% and 61.05% comparing to pure EP.

Table 3: Main parameters collected from CCT of EP and EP/Cy-HEDP system

Sample	EP	EP_5	EP_{10}	EP_{15}
TTI (s)	75	57	59	71
p-HRR (kW/m^2)	1078.4	540.6	438.0	310.9
THR (MJ/m^2)	103.2	83.5	73.4	62.5
p-SPR (m^2/s)	0.32	0.15	0.13	0.11
TSP (m^2/m^2)	22.6	20.2	12.6	8.7
av-COY (kg/kg)	0.0626	0.0510	0.0281	0.0237
Char residue (wt%)	6.9	18.5	30.0	43.8

The production of carbon monoxide (CO) has been provoked as a main toxic gas during combustion. For the av-COY of pure EP, it reaches as high as 0.0626 kg/kg, while that of EP_5, EP_{10} and EP_{15} decreased to 0.0510, 0.0280 and 0.0237 kg/kg, respectively, with the corresponding decrement of 18.5%, 55.4% and 62.2%, indicating lower toxicity of the smoke and higher fire safety of EP/Cy-HEDP composites. From the weight change curves shown as Fig. 6f, the weight of all the EP composites showed a decline tendency during combustion, while the weight of pure EP decreased rapidly, while the descending rate of EP/Cy-HEDP composites is much lower. More excitingly, EP/Cy-HEDP composites show higher char residue yield comparing to the pure EP (6.90 wt%) The char residues of EP_5, EP_{10} and EP_{15} soar to 18.53, 30.04 and 43.76 wt%, respectively. Furthermore, those massive char residues could prevent the exchange of heat and oxygen, therefore epoxy resin composites showing lower heat release and smoke release. As a result, the decline of p-HRR, TSP and CO value as well as the increase of char residue could be explained as follows: On the one hand, during the early stage of combustion, the decomposition products produced by Cy-HEDP promoted the formation of carbon layer on the EP matrix surface, which served as a good physical barrier in condensed phase, blocking heat transfer and reducing the contact between combustible gas and oxygen [36]. On the other hand, the hydrogen and hydroxyl radicals were quenched by phosphorus radicals in the pyrolysis products [37], which could retard and interrupt the combustion.

2.5 Volatile Gases Analysis by TG-IR

To further reveal the fire safety properties, TG-IR was employed to analyze the gas pyrolysis products of pure EP and EP_{15} during thermal decomposition. Figs. 7a and 7b correspondingly depict the FTIR spectra at the initial decomposition temperature (T_d) and the maximum weight loss rate temperature (T_{max}) of pure EP and EP_{15}, respectively. Obviously, the incorporation of Cy-HEDP into EP matrix leads to the reduction of absorbance intensity, indicating the decline of the gaseous products during combustion. There are several common peaks in pure EP and EP_{15} at initial decomposition temperature, such as hydrogen (3587 and 3553 cm^{-1}), carbon dioxide (2384 and 2307 cm^{-1} for EP, 2347 and 2302 cm^{-1} for EP_{15}), carbonyl (1762 and 1790 cm^{-1}) and ether compounds at 1178 cm^{-1}. The peaks at 1508 and 1329 cm^{-1} of EP_{15} refer to the aromatic compounds [38]. Interestingly, the peak (1080 cm^{-1}) representing the stretching vibration of phosphorous compounds, which were considered as the key point to formation of char residual, only appeared during the thermal decomposition of EP_{15}. Meanwhile, the characteristic peak (980 cm^{-1}) of ammonia also appeared in the thermal decomposition of EP_{15}, resulting in the diluting effect. It is evident that the FTIR spectra of gas pyrolysis products of EP and its composites at T_{max} are

similar whereas absorption intensities are different. The lower absorbance intensity indicates the lower pyrolysis products, in other words, lower combustion fuels. This, directly, results the excellent flame retardancy of Cy-HEDP/EP composites.

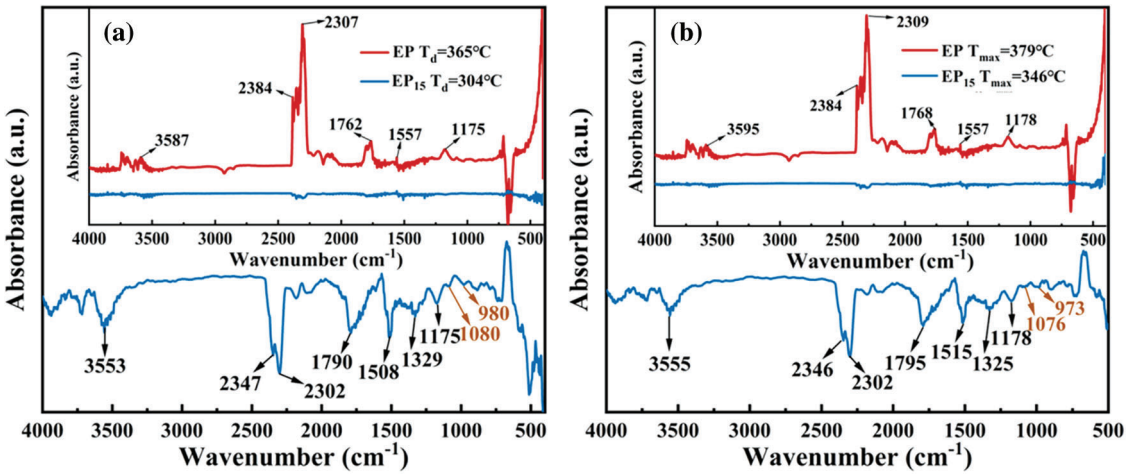

Figure 7: FTIR spectra of gas pyrolysis products of pure EP and EP_{15} at T_d (a) and T_{max} (b)

To better evaluate the gas phase flame-retardant mechanism, the FTIR spectra of pure EP and EP_{15} at different temperature were showed in Figs. 8a and 8b. The major products of pure EP and EP_{15} are similar including hydrogen (3595 and 3555 cm^{-1}), carbon dioxide (2384 and 2309 cm^{-1} for EP, 2346 and 2302 cm^{-1} for EP_{15}), carbonyl (1768 and 1795 cm^{-1}) and ether compounds at 1178 cm^{-1}, whereas absorption intensity of EP_{15} is much lower than that of EP. The EP/Cy-HEDP thermosets began to release pyrolysis products earlier than pure EP, indicating the addition of Cy-HEDP can catalyze the thermal decomposition of EP matrix. The intensity of CO_2 peak is relatively higher than that of pure EP at high temperature, which could dilute the flammable gas and oxygen in the gas phase, thereby slowing down or disturbing the combustion. On the other hand, the high yield of CO_2 contributes to more char residual in the condensed phase. Furthermore, the peak intensity of gas products such as carbonyl and ether compounds for EP/Cy-HEDP are weak than that of pure EP, showing a lower toxic gas production during combustion.

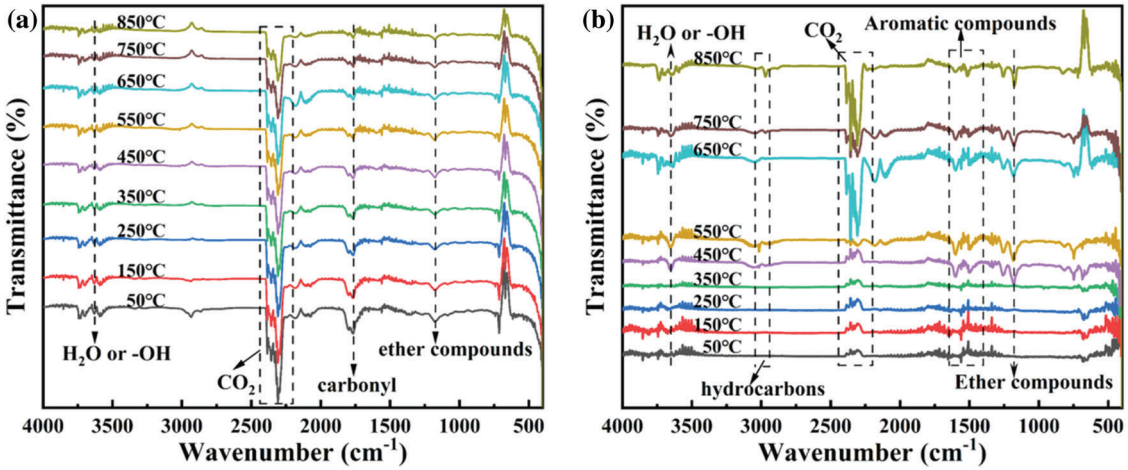

Figure 8: FTIR spectra of the gas pyrolysis products of pure EP (a) and EP_{15} (b) at different temperatures

2.6 Char Residue Analysis

In order to reveal the condensed-phased products of EP composites during combustion, the photograph and microcosmic views of char residues after CCT test were recorded by digital camera and SEM. As can be seen in Fig. 9, the char residues of pure EP are fragile and loose, which is not helpful to protect the EP matrix. When the Cy-HEDP was incorporated into EP, the char residual of EP_{15} after combustion evidently increased, and the char layers become compact and continuous.

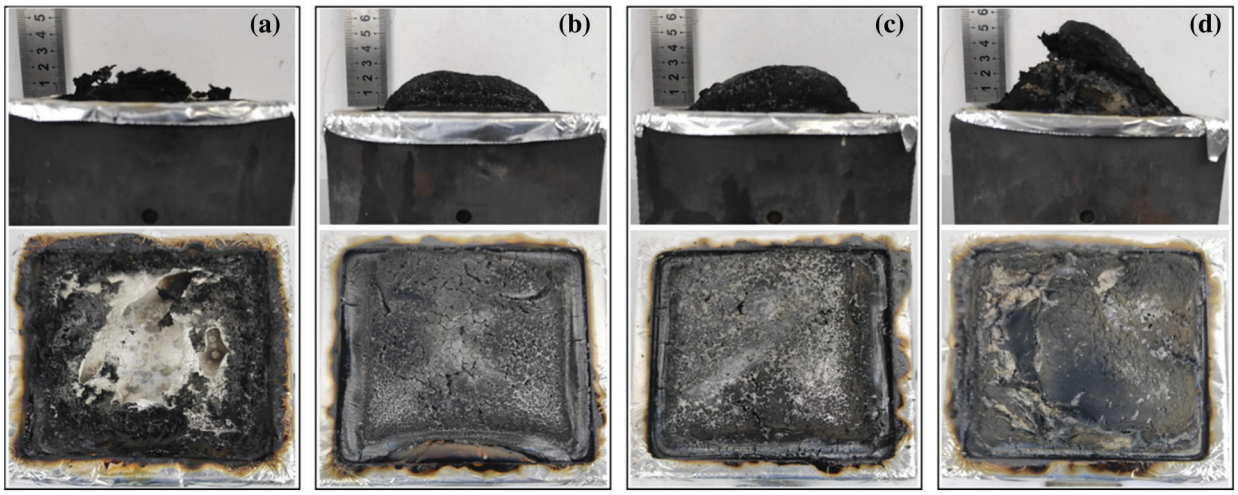

Figure 9: Digital photos of pure EP (a), EP_5 (b), EP_{10} (c), EP_{15} (d) after CCT

From the results of SEM images, as shown in Fig. 10, it can be clearly found that lots of cracks on the char residue surface of pure EP. In contrast, EP/Cy-HEDP composites exhibit continuous and compact char layers with only few small holes. It is inferred that the compact and continuous char layers contribute to fewer smoke production and heat release of EP/Cy-HEDP composites during combustion through exerting barrier effect.

Raman spectrum was utilized to further investigate the graphitization degree of char residues. Fig. 11 exhibits the Raman spectra of pure EP and EP_{15}. There are two typical peaks at 1360 and 1590 cm^{-1}, which correspondingly presented the D-band and G-band. The D-band reflects the content of defective carbon in carbon materials, and the G-band reflects the content of graphitized carbon in the carbon materials. Generally, the lower the ID/IG value, the higher the graphitization degree. It is believed that higher degree of graphitization leads to higher strength of the char layers, which can effectively act as a barrier to the oxygen and flammable gas during the combustion. The I_D/I_G value of pure EP is 2.71, while that of EP_{15} descends to 2.49, which indicates that the addition of Cy-HEDP contributes to the formation of graphitized carbon during combustion.

2.7 Potential Flame-Retardant Mechanism

Fig. 12 depicts a diagrammatic sketch of the possible flame-retardant mechanism, which can be divided into gas phase and condensed phase. The probably mechanism is proposed as follows: (i) The EP/Cy-HEDP composite produce nonflammable gases such as carbon dioxide, water vapor and ammonia, which can dilute the concentration of combustible gases and oxygen [39,40] even extinguish the flame. (ii) The carbonization effect of Cy-HEDP plays a synergistic role in acquiring dense and continuous char layers, affording better shielding action and protecting the EP matrix from further combustion. (iii) The phosphorus components from HEDP can produce phosphorus free radicals (P· or PO·) that could interrupt the combustion process

by quenching H· or HO· radicals [41,42]. In conclusion, the incorporation of bio-based Cy-HEDP can give scope to flame retardant effect among EP composites both in gas phase and condensed phase.

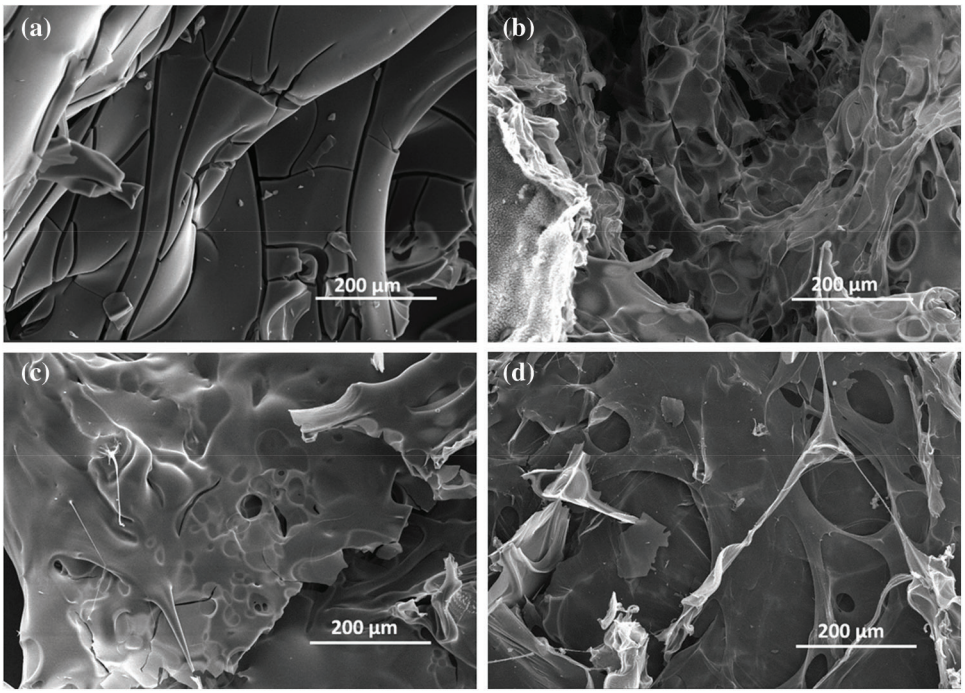

Figure 10: SEM images of pure EP (a), EP_5 (b), EP_{10} (c), EP_{15} (d) after CCT

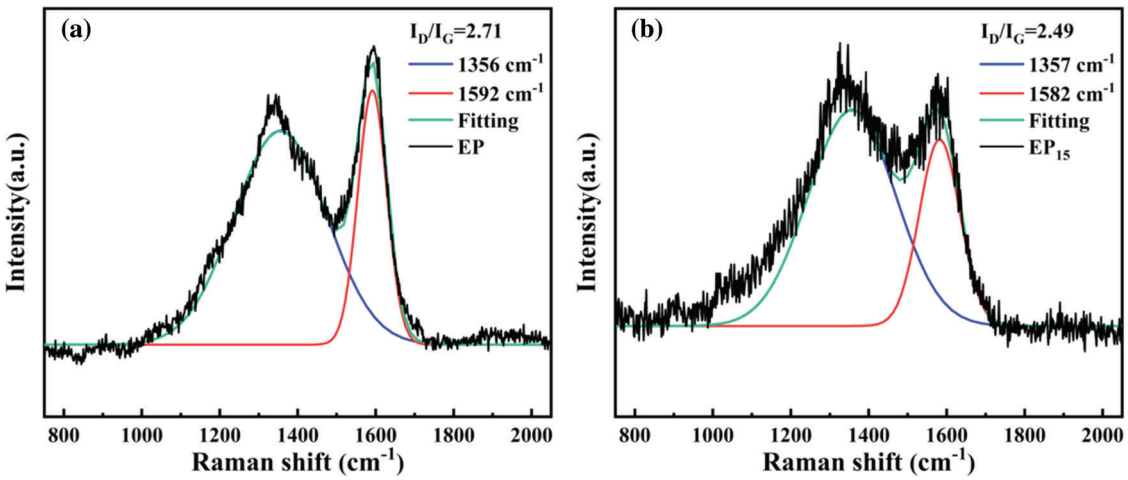

Figure 11: Raman spectrums of pure EP (a) and EP_{15} (b)

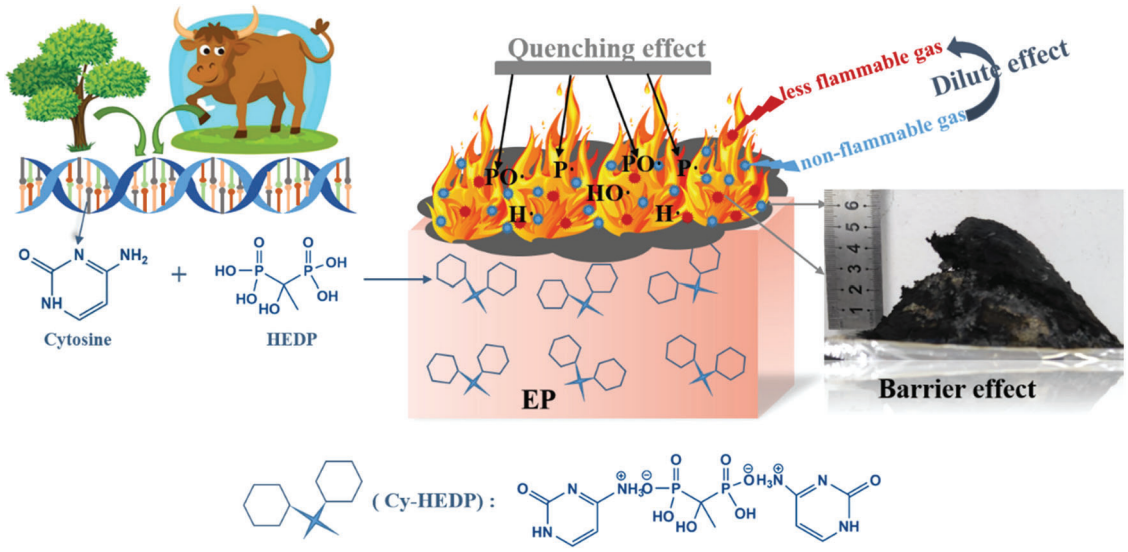

Figure 12: Possible mechanism of Cy-HEDP in EP

3 Conclusion

In this work, the bio-based Cy-HEDP was successfully synthesized through a facile and economical salt-forming reaction, the final product was investigated by FTIR, NMR, SEM and XPS. With the addition of 15 wt% Cy-HEDP, EP_{15} can pass the UL-94 V-0 rating with the LOI of 28.5%. Compared to pure EP, the total smoke production (TSP) as well as total heat release (THR) of EP_{15} decreased by 61.05% (from 22.61 to 8.7 m^2/m^2) and 39.44% (from 103.19 to 62.50 MJ/m^2), respectively. From the analysis of gas product during combustion and residual char, it can be concluded that EP/Cy-HEDP composites can release more nonflammable gases to dilute the combustible gases and oxygen, as well as contribute to more condensed and continuous char layers, protecting EP matrix from further combustion. Overall, Cy-HEDP can simultaneously endow epoxy matrix with excellent flame retardancy and smoke toxicity suppression performance.

Acknowledgement: We gratefully acknowledge the financial supports from Fundamental Research Funds for the Central Universities (2020CDJQY-A006), the National Natural Science Foundation of China (No. 51603025), The Opening Fund of State Key Laboratory of Fire Science (HZ2019-KF11).

Funding Statement: The authors received no specific funding for this study.

Conflicts of Interest: The authors declare that they have no conflicts of interest to report regarding the present study.

References

1. Zhu, Y., Di, B., Chen, H., Wang, X., Tian, Y. (2019). *In situ* synthesis of novel biomass lignin/silica based epoxy resin adhesive from renewable resources at different pHs. *Journal of Adhesion Science and Technology, 33(16),* 1806–1820. DOI 10.1080/01694243.2019.1617511.
2. Scarselli, G., Corcione, C., Nicassio, F., Maffezzoli, A. (2017). Adhesive joints with improved mechanical properties for aerospace applications. *International Journal of Adhesion and Adhesives, 75,* 174–180. DOI 10.1016/j.ijadhadh.2017.03.012.
3. Jin, Y., Liu, J., Xie, X., Zhai, L. (2018). Different effects of steel fiber and nano-SiO_2 on epoxy resin concrete. *IOP Conference Series: Earth and Environmental Science, 186(2),* 12040. DOI 10.1088/1755-1315/186/2/012040.

4. Fischer, J., Bradler, P. R., Schmidtbauer, D., Lang, R. W., Wan-Wendner, R. (2019). Long-term creep behavior of resin-based polymers in the construction industry. *Materials Today Communications, 18,* 60–65. DOI 10.1016/j.mtcomm.2018.11.006.
5. Hu, D., Zhang, X., Liu, X., Qin, Z., Hu, L. et al. (2020). Study on toughness improvement of a rosin-sourced epoxy matrix composite for green aerospace application. *Journal of Composites Science, 4(4),* 168. DOI 10.3390/jcs4040168.
6. Zhang, S., Xie, Z., Peng, Z. (2021). Space charge characteristics in epoxy resin impregnated paper under AC and AC-DC superimposed electric fields. *IEEE Transactions on Dielectrics and Electrical Insulation, 28(2),* 381–389. DOI 10.1109/TDEI.2020.009162.
7. Dai, X., Li, P., Sui, Y., Zhang, C. (2021). Thermal and flame-retardant properties of intrinsic flame-retardant epoxy resin containing biphenyl structures and phosphorus. *European Polymer Journal, 147,* 110319. DOI 10.1016/j.eurpolymj.2021.110319.
8. Li, X., Zhang, J., Zhang, L., de Luzuriaga, A. R., Rekondo, A. et al. (2021). Recyclable flame-retardant epoxy composites based on disulfide bonds: Flammability and recyclability. *Composites Communications, 25,* 100754. DOI 10.1016/j.coco.2021.100754.
9. Zhang, Y., Li, L., Shi, D., Song, F. (2021). Synthesis and application of low-cost layered double hydroxides intercalated by gluconic acid anion for flame retardancy and tensile strength conservation of high filling epoxy resin. *Journal of Colloid and Interface Science, 594,* 791–801. DOI 10.1016/j.jcis.2021.03.088.
10. Cheng, C., Yan, J., Lu, Y., Ma, W., Li, C. et al. (2021). Effect of chitosan/lignosulfonate microencapsulated red phosphorus on fire performance of epoxy resin. *Thermochimica Acta, 700,* 178931. DOI 10.1016/j.tca.2021.178931.
11. Sun, J., Wu, Z., An, B., Ma, C., Xu, L. et al. (2021). Thermal-insulating, flame-retardant and mechanically resistant aerogel based on bio-inspired tubular cellulose. *Composites Part B: Engineering, 220,* 108997. DOI 10.1016/j.compositesb.2021.108997.
12. Li, X., Zhang, F., Jian, R., Ai, Y., Ma, J. et al. (2019). Influence of eco-friendly calcium gluconate on the intumescent flame-retardant epoxy resin: Flame retardancy, smoke suppression and mechanical properties. *Composites Part B: Engineering, 176,* 107200. DOI 10.1016/j.compositesb.2019.107200.
13. Wang, N., Gao, H., Zhang, J., Qin, Y., Wang, D. (2019). Phytic acid intercalated graphene oxide for anticorrosive reinforcement of waterborne epoxy resin coating. *Polymers, 11(12),* 1950. DOI 10.3390/polym11121950.
14. Gao, Y., Deng, C., Du, Y., Huang, S., Wang, Y. (2019). A novel bio-based flame retardant for polypropylene from phytic acid. *Polymer Degradation and Stability, 161,* 298–308. DOI 10.1016/j.polymdegradstab.2019.02.005.
15. Wang, H., Cao, M., Zhao, H., Liu, J., Geng, C. et al. (2020). Double-cross-linked aerogels towards ultrahigh mechanical properties and thermal insulation at extreme environment. *Chemical Engineering Journal, 399,* 125698. DOI 10.1016/j.cej.2020.125698.
16. Nabipour, H., Wang, X., Song, L., Hu, Y. (2020). A fully bio-based coating made from alginate, chitosan and hydroxyapatite for protecting flexible polyurethane foam from fire. *Carbohydrate Polymers, 246,* 116641. DOI 10.1016/j.carbpol.2020.116641.
17. Yu, G., Ma, C., Li, J. (2020). Flame retardant effect of cytosine pyrophosphate and pentaerythritol on polypropylene. *Composites Part B: Engineering, 180,* 107520. DOI 10.1016/j.compositesb.2019.107520.
18. Yu, Y., Fu, S., Song, P. A., Luo, X., Jin, Y. et al. (2012). Functionalized lignin by grafting phosphorus-nitrogen improves the thermal stability and flame retardancy of polypropylene. *Polymer Degradation and Stability, 97(4),* 541–546. DOI 10.1016/j.polymdegradstab.2012.01.020.
19. Battegazzore, D., Alongi, J., Fontaine, G., Frache, A., Bourbigot, S. et al. (2015). Bulk *vs.* surface flame retardancy of fully bio-based polyamide 10,10. *RSC Advances, 5(49),* 39424–39432. DOI 10.1039/C5RA04149J.
20. Xu, X., Wang, S., Ma, S., Yuan, W., Li, Q. et al. (2019). Vanillin-derived phosphorus-containing compounds and ammonium polyphosphate as green fire-resistant systems for epoxy resins with balanced properties. *Polymers for Advanced Technologies, 30(2),* 264–278. DOI 10.1002/pat.4461.
21. Jia, Y., Hu, Y., Zheng, D., Zhang, G., Zhang, F. et al. (2017). Synthesis and evaluation of an efficient, durable, and environmentally friendly flame retardant for cotton. *Cellulose, 24(2),* 1159–1170. DOI 10.1007/s10570-016-1163-z.

22. Howell, B. A., Alrubayyi, A., Ostrander, E. A. (2019). Thermal properties of charring plasticizers from the biobased alcohols, pentaerythritol and 3, 5-dihydroxybenzoic acid. *Journal of Thermal Analysis and Calorimetry, 138(4),* 2661–2668. DOI 10.1007/s10973-019-08311-8.
23. Shi, X., Ju, Y., Zhang, M., Wang, X. (2018). The intumescent flame-retardant biocomposites of poly(lactic acid) containing surface-coated ammonium polyphosphate and distiller's dried grains with solubles (DDGS). *Fire and Materials, 42(2),* 190–197. DOI 10.1002/fam.2479.
24. Guan, Y., Huang, J., Yang, J., Shao, Z., Wang, Y. (2015). An effective Way to flame-retard biocomposite with ethanolamine modified ammonium polyphosphate and its flame retardant mechanisms. *Industrial & Engineering Chemistry Research, 54(13),* 3524–3531. DOI 10.1021/acs.iecr.5b00123.
25. Hu, X., Yang, H., Jiang, Y., He, H., Liu, H. et al. (2019). Facile synthesis of a novel transparent hyperbranched phosphorous/nitrogen-containing flame retardant and its application in reducing the fire hazard of epoxy resin. *Journal of Hazardous Materials, 379,* 120793. DOI 10.1016/j.jhazmat.2019.120793.
26. Yu, G., Ma, C., Li, J. (2020). Flame retardant effect of cytosine pyrophosphate and pentaerythritol on polypropylene. *Composites Part B: Engineering, 180,* 107520. DOI 10.1016/j.compositesb.2019.107520.
27. Chen, S., Wu, F., Hu, Y., Lin, S., Yu, C. et al. (2020). A fully bio-based intumescent flame retardant for poly (butylene succinate). *Materials Chemistry and Physics, 252,* 123222. DOI 10.1016/j.matchemphys.2020.123222.
28. Liu, L., Xu, Y., Xu, M., Li, Z., Hu, Y. et al. (2019). Economical and facile synthesis of a highly efficient flame retardant for simultaneous improvement of fire retardancy, smoke suppression and moisture resistance of epoxy resins. *Composites Part B: Engineering, 167,* 422–433. DOI 10.1016/j.compositesb.2019.03.017.
29. Gao, Y., Deng, C., Du, Y., Huang, S., Wang, Y. (2019). A novel bio-based flame retardant for polypropylene from phytic acid. *Polymer Degradation and Stability, 161,* 298–308. DOI 10.1016/j.polymdegradstab.2019.02.005.
30. Nabipour, H., Wang, X., Song, L., Hu, Y. (2020). A fully bio-based coating made from alginate, chitosan and hydroxyapatite for protecting flexible polyurethane foam from fire. *Carbohydrate Polymers, 246,* 116641. DOI 10.1016/j.carbpol.2020.116641.
31. Zhang, T., Yan, H., Shen, L., Fang, Z., Zhang, X. et al. (2014). Chitosan/Phytic acid polyelectrolyte complex: A green and renewable intumescent flame retardant system for ethylene–Vinyl acetate copolymer. *Industrial & Engineering Chemistry Research, 53(49),* 19199–19207. DOI 10.1021/ie503421f.
32. Andriy, L. P., Svitlana, P. S., Andriy, V. S., Dmytro, M. H. (2003). Unusual behavior of cytosine aminogroup signal in ^{1}H NMR spectra in DMSO depending on its concentration. *Proceedings of XVI International Conference on Spectroscopy of Molecules and Crystals,* vol. 5507, pp. 140–147. DOI 10.1117/12.569624.
33. Wang, W., Yuan, Y., Yu, B., Liew, K. M., Yuen, R. K. K. et al. (2020). Controlled self-template synthesis of manganese-based cuprous oxide nanoplates towards improved fire safety properties of epoxy composites. *Journal of Hazardous Materials, 387,* 122006. DOI 10.1016/j.jhazmat.2019.122006.
34. Yuan, Y., Shi, Y., Yu, B., Zhan, J., Zhang, Y. et al. (2020). Facile synthesis of aluminum branched oligo (phenylphosphonate) submicro-particles with enhanced flame retardance and smoke toxicity suppression for epoxy resin composites. *Journal of Hazardous Materials, 381,* 121233. DOI 10.1016/j.jhazmat.2019.121233.
35. Costes, L., Laoutid, F., Brohez, S., Dubois, P. (2017). Bio-based flame retardants: When nature meets fire protection. *Materials Science and Engineering: R: Reports, 117,* 1–25. DOI 10.1016/j.mser.2017.04.001.
36. Wang, W., Yuan, Y., Yu, B., Liew, K. M., Yuen, R. K. K. et al. (2020). Controlled self-template synthesis of manganese-based cuprous oxide nanoplates towards improved fire safety properties of epoxy composites. *Journal of Hazardous Materials, 387,* 122006. DOI 10.1016/j.jhazmat.2019.122006.
37. Mariappan, T., Zhou, Y., Hao, J., Wilkie, C. A. (2013). Influence of oxidation state of phosphorus on the thermal and flammability of polyurea and epoxy resin. *European Polymer Journal, 49(10),* 3171–3180. DOI 10.1016/j.eurpolymj.2013.06.009.
38. Xie, W., Huang, S., Tang, D., Liu, S., Zhao, J. (2020). Biomass-derived Schiff base compound enabled fire-safe epoxy thermoset with excellent mechanical properties and high glass transition temperature. *Chemical Engineering Journal, 394,* 123667. DOI 10.1016/j.cej.2019.123667.
39. Wang, H., Liu, Q., Zhao, X., Jin, Z. (2021). Synthesis of reactive DOPO-based flame retardant and its application in polyurethane elastomers. *Polymer Degradation and Stability, 183,* 109440. DOI 10.1016/j.polymdegradstab.2020.109440.

40. Yang, S., Huo, S., Wang, J., Zhang, B., Wang, J. et al. (2021). A highly fire-safe and smoke-suppressive single-component epoxy resin with switchable curing temperature and rapid curing rate. *Composites Part B: Engineering, 207,* 108601. DOI 10.1016/j.compositesb.2020.108601.
41. Costes, L., Laoutid, F., Brohez, S., Dubois, P. (2017). Bio-based flame retardants: When nature meets fire protection. *Materials Science and Engineering: R: Reports, 117,* 1–25. DOI 10.1016/j.mser.2017.04.001.
42. Liang, S., Hemberger, P., Neisius, N. M., Bodi, A., Grützmacher, H. et al. (2015). Elucidating the thermal decomposition of dimethyl methylphosphonate by vacuum ultraviolet (VUV) photoionization: Pathways to the PO radical, a Key species in flame-retardant mechanisms. *Chemistry, 21(3),* 1073–1080. DOI 10.1002/chem.201404271.